10th International Conference on Contact Mechanics
CM2015, Colorado Springs, Colorado, USA

Ratcheting and Wear Behavior of Australian Rail Steel: Experimental Investigation of Material Properties and Sampling Method

Asitha C. Athukorala
Queensland University of Technology
Brisbane, QLD 4000, Australia
asitha.athukoralalage@qut.edu.au

Dennis V. De Pellegrin
Queensland University of Technology
Brisbane, QLD 4000, Australia

Kyriakos I. Kourousis
University of Limerick
Castletroy, Co. Limerick, Ireland

ABSTRACT

To The ratcheting behavior of high-strength rail steel (Australian Standard AS1085.1) is studied in this work for the purpose of predicting wear and damage to the rail surface. Historically, researchers have used circular test coupons obtained from the rail head to conduct cyclic load tests, but according to hardness profile data, considerable variation exists across the rail head section. For example, the induction-hardened rail (AS1085.1) shows high hardness (400-430 HV100) up to four-millimeters into the rail head's surface, but then drops considerably beyond that. Given that cyclic test coupons five millimeters in diameter at the gauge area are usually taken from the rail sample, there is a high probability that the original surface properties of the rail do not apply across the entire test coupon and, therefore, data representing only average material properties are obtained. In the literature, disks (47 mm in diameter) for a twin-disk rolling contact test machine have been obtained directly from the rail sample and used to validate rolling contact fatigue wear models. The question arises: How accurate are such predictions? In this research paper, the effect of rail sampling position on the ratcheting behavior of AS1085.1 rail steel was investigated using rectangular shaped specimens. Uniaxial stress-controlled tests were conducted with samples obtained at four different depths to observe the ratcheting behaviour of each. Micro-hardness measurements of the test coupons were carried out to obtain a constitutive relationship to predict the effect of depth on the ratcheting behaviour of the rail material. This work ultimately assists the selection of valid material parameters for constitutive models in the study of rail surface ratcheting.

Keywords—ratcheting; rail steel; hardness; pearlite

1. Introduction

Railway systems play a crucial role in many countries in terms of social and economic development, especially countries like Australia, Canada, USA, South Africa and China which have mining driven economies. Australian heavy-haul, intermodal and freight rail expertise is broad and diverse. Australia operates (Fortescue Metals Group Ltd) the largest heavy-haul train in the world with axle loads of 40-tonnes and a trailing load of 35200-tonnes operating 24 hours a day [1]. In comparison, the United States of America, Canada and China have trailing loads of 22000, 20700 and 20000 tonnes respectively, with axle loads under 30 tonnes. BHP Billiton in the Pilbara region of Western Australia runs iron-ore trains at 40-tonnes axle load on 68 kg/m rails, with maximum speed of 75 km/h. In order to maintain such high levels of performance, the quality of rail materials is very important for reducing wear and other forms of rail deterioration.

In Australia, high-strength hypereutectoid steel rail material is used according to Australian Standards specification AS1085.1 and exhibiting hardness in the range 360-420HV at the railhead. The material specification aims to provide better performance but it appears that field performance of the material hasn't been studied comprehensively.

Rails are subjected to repetitive loads and the damage mechanism is governed by plastic deformation of the rail surface. This phenomenon is also known as cyclic plasticity. Different positions of the rail are

subjected to varying stress and strain conditions. Under stress-controlled cyclic behaviour, accumulation of plastic deformation called ratcheting takes place. The accumulated plastic strain is called the ratcheting strain.

Good material modelling helps to make better predictions on rolling contact fatigue and wear at the rail wheel contact. The material parameters used in material modelling may be obtained through stress- and strain-controlled testing. Numerous researchers have carried out investigations on fatigue life and both the hardening and softening effects of materials under varying conditions of mean stress, amplitude and preloading conditions.

In 2013, Pun et al. [2] performed an experimental study on the cyclic deformation characteristics and

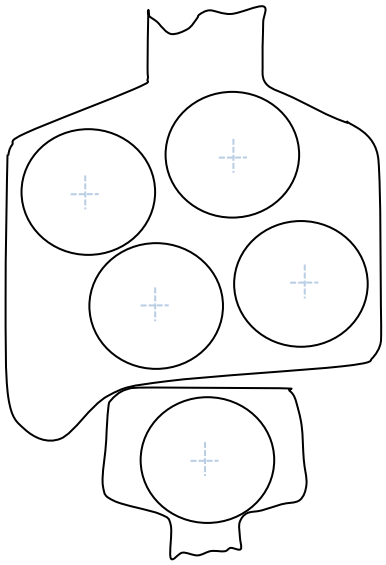

Fig. 1. Rail and wheel sampling positions [7].

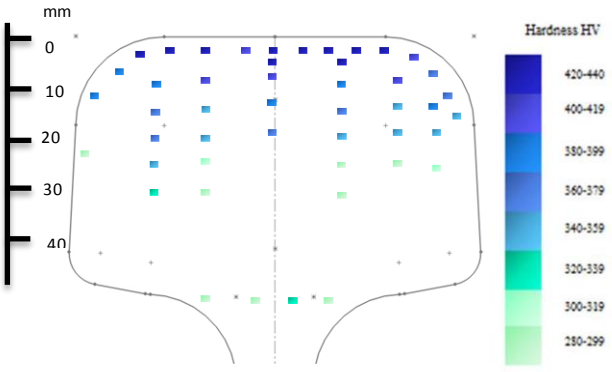

Fig. 2. Vickers hardness (HV100) profile of the rail-head.

ratcheting behaviour of hypereutectoid high-strength rail steel which is used in the Australian heavy-haul industry. They conducted tests on 68 kg/m rail sample – it is worth bearing in mind that 50 and 60 kg/m rails are also commonly used in the industry [3]. Although Pun et al.'s study was limited to a low number of cycles (100 cycles typically), it was discovered that kinematic hardening is dominant in the ratcheting of the material.

Some researchers [4-8] have used material models to predict rail wear and the formation of other defects in the rail-wheel contact interface. The small twin-disk machines (SUROS and LEROS) used rail disks which were obtained from rail and wheel samples [7-9] as illustrated in Fig. 1. The results generated from the twin-disk machine tests using these wheels were subsequently adapted to validate the relevant wear simulation models.

From the present authors' work, hardness varies across the section of a head hardened rail in the fashion typically shown in Fig. 2. According to the distribution profile, rail hardness reduces considerably as depth increases. Thus, it is evident that errors will arise in the prediction of wear and ratcheting behaviour of the rail-head surface due to the varying material hardness likely to be exhibited over the surface of any test wheels.

A problem also arises with material modelling when cyclic load tests are used to determine the parameters of a material model. Many researchers [10, 11] use circular-section samples which are acceptable for homogenous materials. But head-hardened rail materials are subjected to an induction hardening process which may result in different properties as each test-coupon is acquired from a different location in the rail cross-section.

For example, one researcher used circular test coupons 10 mm in diameter narrowing to a 5 mm gauge diameter [3]. But, according to the material hardness profile, there is a good chance of missing the original material properties at the rail surface, thus, leading to inaccurate data.

In this paper, the limitation and effects of the sampling depth on the ratcheting parameters of the rail steel are investigated. The ultimate objective is to use this information to make corrections to rail test-rig simulations (where disk samples are obtained from the rail head) to obtain better predictions of material properties and behaviour.

2. Experimental Approach

2.1. Material

The material tested was cut from new 60 kg/m, grade AS1085.1 rail, with chemical composition given in Table I. The material microstructure was studied at different depths in both transverse and longitudinal directions. The transverse section shows that the microstructure changes from fine pearlite to a coarse

Table I. Chemical Composition

Element	Composition
C	0.7% - 0.82%
Mn	0.7% - 1.1%
P	0.04%
S	0.04%
Si	0.1% – 0.35%

pearlite structure with increasing depth. Grain distortion in the worked direction and inclusions can be observed in the longitudinal section due to the hot rolling process.

2.2. Sample Location

As rail steel material properties vary along the cross-section of the head, it is important to select the sampling volume with care. Sampling positions were chosen according to the hardness profile and practical considerations necessary for cutting the samples from the rail head. As shown in Fig. 3, the top sample is very close to the rail-head surface while the fourth sample is 33 mm below the rail surface. According to the hardness profile (Fig. 2), the 1-5 mm layer exhibits high hardness (410-430 HV), which then drops significantly as the depth increases.

Rectangular-shaped test coupons (according to ASTM E466 specification) were obtained from each sampling location. The dimensions of the test coupon are shown in Fig. 4.

An MTS 810 cyclic testing machine designed to perform force- and displacement-controlled tests was used to conduct the experiments on the rectangular-shaped specimens. A major problem with the rectangular shape is that the test coupon can buckle when subjected to compression during cyclic-load testing. The rectangular specimens were therefore designed and machined with a low slenderness-ratio in order to avoid such effect.

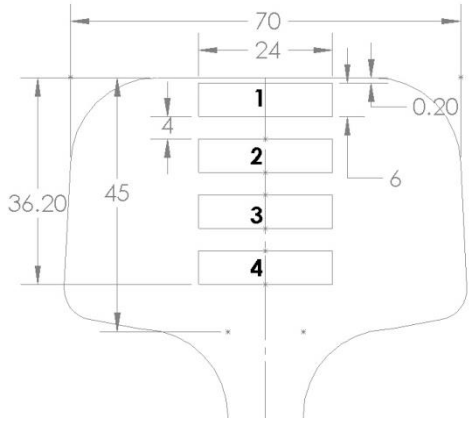

Fig. 3. Sampling position of the rail head.

Trial specimens were tested before the actual tests were designed. The aim of these trials was to test that the hydraulic grips of the MTS 810 were capable of sufficient grip pressure so as to avoid slipping at high-load conditions. The knife-edge extensometer was also tested to ensure that good contact was always maintained between the surface of specimen and the knife edges. Good contact, without any slip, is necessary for accurate strain measurement.

The test coupons were machined with a gauge length of 21 mm and rectangular cross-section dimensions of 6 mm by 10 mm. Before testing, the gauge surfaces of each test piece were ground and polished to mirror-like finish, free from scratches visible to the naked eye. This process was conducted to prevent crack initiation and premature failure due to surface defects.

2.3. Fatigue Tests

Force-control tests were performed using the MTS 810 with TestStar II® control system, in accordance with standard ASTM E466 [12]. All test coupons were subjected to the same uniaxial force-controlled test by keeping the amplitude and mean constant in order to study the ratcheting behaviour of each test coupon.

The uniaxial cyclic force-controlled test method used a triangular waveform and the axial load was

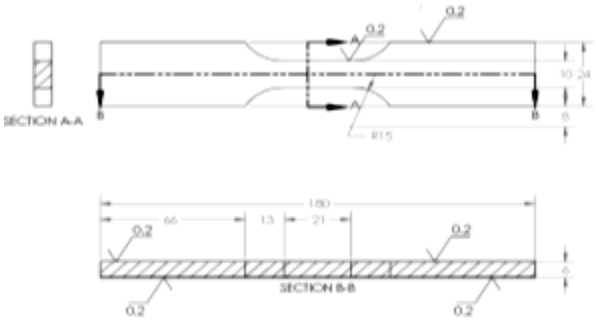

Fig. 4. Rectangular test coupon dimension.

controlled by means of load-cell feedback. During each test, the axial load rate was maintained at 8.5 kN/s – equivalent to a stress rate of 140 MPa/s. A mean stress of 83 MPa and stress amplitude of 694 MPa were used. Cyclic loading was carried out until stabilization of the ratcheting cycle or reaching the critical strain level (0.1).

3. Results and Discussion

3.1. Microstructure of Rail Steel

The rail microstructures have been identified as ferrite and cementite layers of varying refinement. Due to induction hardening, different pearlites and upper bainitic microstructures exist. As shown in Fig. 5, the microstructure varies both in longitudinal and

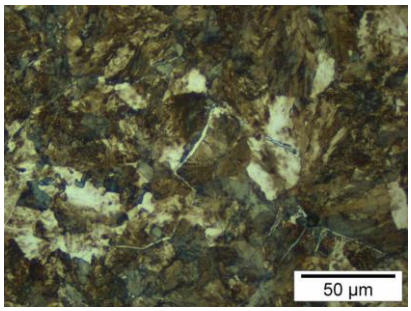

a) Transverse section (0.2 mm depth)

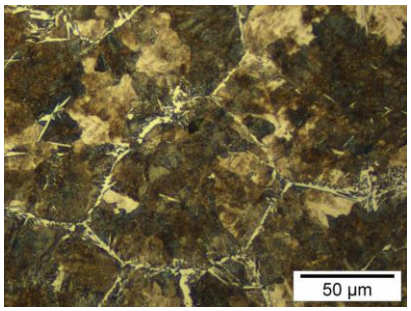

b) Longitudinal section (0.2 mm depth)

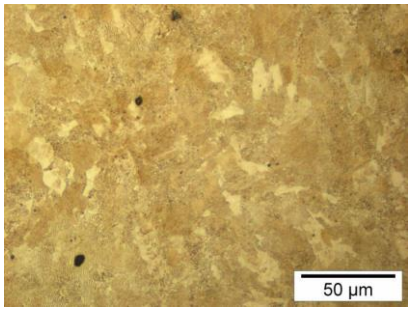

c) Transverse section (32 mm depth)

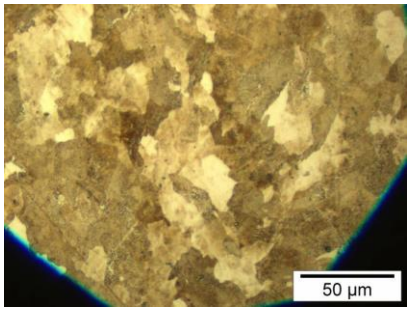

d) Longitudinal section (32 mm depth)

Fig. 5. Microstructure of the rail head for longitudinal and transverse cross-sections at two different depths.

transverse directions. Near the rail surface (0.2 mm depth), more ferrite precipitation exists at the grain boundary, and the darker region in Fig. 5(a) represents an upper bainitic microstructure. To aid visualisation of the microstructure the polished surfaces were etched with 3% nital.

3.2. Stress-Controlled Test

The rectangular-shaped specimens obtained from the rail at different depth levels were tested under the same conditions; i.e. uniaxial, symmetrical stress-control, at room temperature with predefined stress amplitude and mean. Close observation of the tensile stress-strain curves in Fig. 6 shows distinct variation of the sample elongation in the first load cycle. For example, the level 4 sample exhibited about five-time greater elongation than the level 1 (top) sample. Also, yield stress diminishes with increasing depth; the bottom test coupon yield stress is 31% less than the top test coupon.

Strain amplitude variation is plotted in Fig. 7 and it may be clearly observed that strain amplitude is higher at greater depth, under otherwise identical test conditions. The material becomes weaker with depth and exhibits greater tendency to deform plastically. The first two specimens exhibit a plateau in the strain amplitude as the material properties stabilize with further loading cycles.

The strain amplitudes of level 1 and 2 test coupons' plateau after about 5 and 10 cycle respectively due to

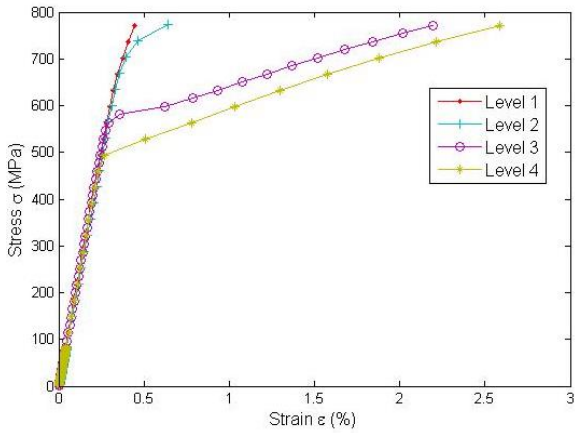

Fig. 6. Tensile stress and strain behaviour of specimens at different depths (refer Fig. 3) from the surface.

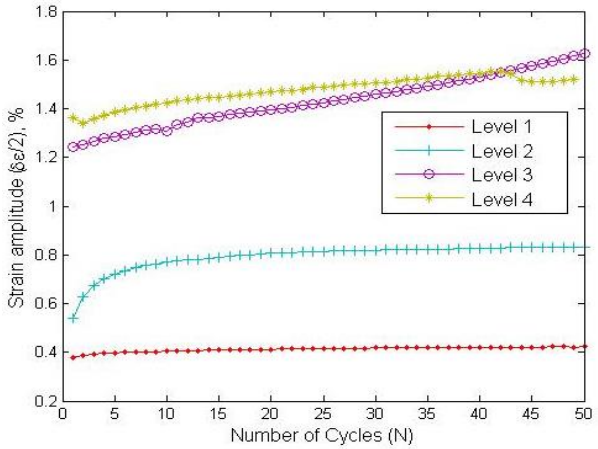

Fig. 7. Strain amplitude at different depths (refer Fig. 3) versus number of cycles.

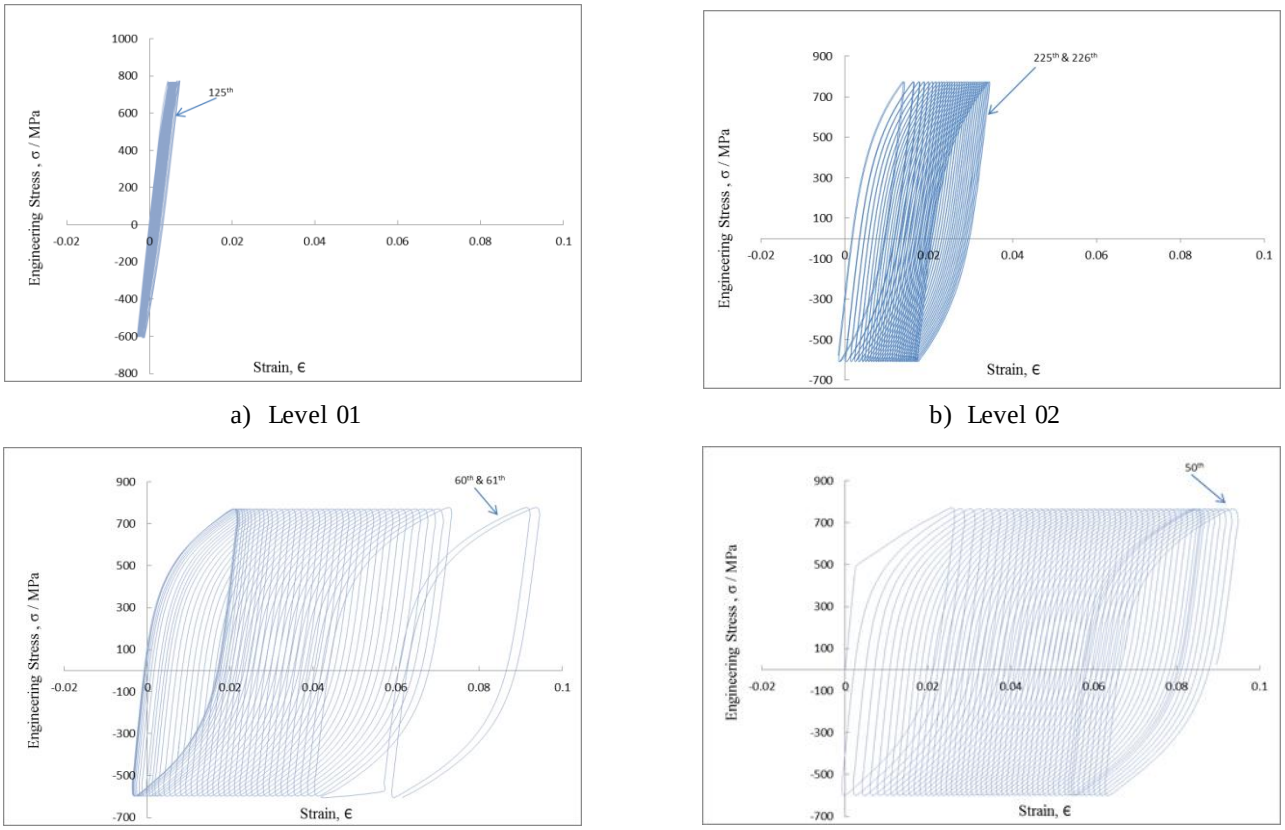

a) Level 01 b) Level 02

c) Level 03 d) Level 04

Fig. 8. Stress-strain curve for the different sampling depths (refer Fig. 3).

cyclic hardening and stabilisation of ratcheting behaviour. There appears to be no stabilisation with the other two test coupons as the strain amplitude continues to grow (softening effect) with increasing number of cycles.

Furthermore, the level 1 test coupon shows a small hysteresis loop area compared to the level 4 coupon; the latter absorbing far greater strain energy due to the increased nucleation and mobility of dislocations. Each test exhibited a smaller hysteresis curve area in the beginning which gradually expands as the number of cycles progresses; this may be explained by the fact that plastic deformation in the test coupon initially occurs locally and then gradually expands throughout the gauge volume. Furthermore, the level 1 test coupon shows a small hysteresis loop area compared to the level 4 coupon; the latter absorbing far greater strain energy due to the increased nucleation and mobility of dislocations. Each test exhibited a smaller hysteresis curve area in the beginning which gradually expands as the number of cycles progresses; this may be explained by the fact that plastic deformation in the test coupon initially occurs locally and then gradually expands throughout the gauge volume.

The experimental cyclic stress-strain data is shown in Fig. 8 and illustrates the very different softening and hardening behaviour of the rail steel at different depth under the same force-controlled conditions.

Furthermore, it can be observed that the first and second test coupons exhibited strain hardening behaviour as the hysteresis loops contracted with increasing number of cycles, while the level 3 coupon loops expanded with cycles suggesting softening behaviour. Level 4 showed cyclic hardening initially with increasing strain amplitude until 42nd cycles and then start softening the material. This could be due to some induction effect as level 4 is close to outer surface.

The microstructure of the rail steel varied with the depth, in top layer it has a mix of bainitic and pearlitic structures (Fig. 5a) while the bottom layer has fine pearlitic structure (Fig. 5c). A tendency towards hardening is observed near the top and softening behaviour is observed in the lower test coupons. This is consistent with Sunwoo's research [13] – i.e. steel with fine pearlite structure is softer when compared to combined bainitic and pearlitic structures.

Ratcheting curves for each depth level are shown in Fig. 9. Higher ratcheting strain is observed corresponding to increased depth under the same force controlled test conditions. The bottom two test coupons

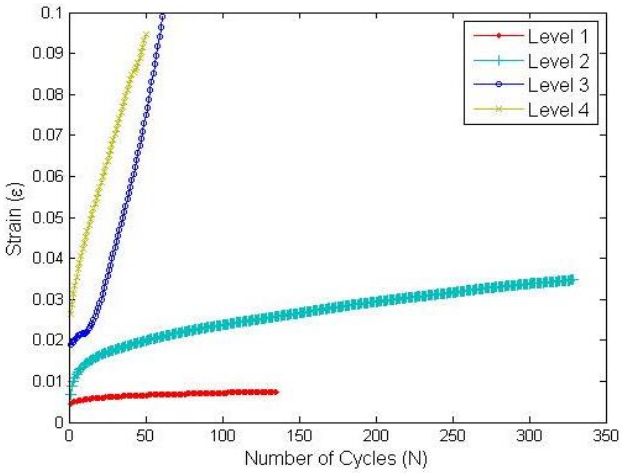

Fig. 9. Ratcheting curves for each test coupons.

exhibit high ratcheting rates leading to failure after relatively few loading cycles.

All the graphs highlight an important trait of head hardened rail steel: after a certain depth from the rail surface (between second and third coupons in this instance) there is a transition in material ratcheting behaviour attributed to microstructural differences arising from the induction hardening process.

Ratcheting is an important mechanism in rail wear, crack initiation and development. These cyclic load tests results give how material at different depths from the surface of the rail behave under cyclic loads which induce significant plastic deformations.

Samples obtained from the rail sections by Tyfour et al. [7, 8] had a high likelihood of material property inhomogeneity. When the sample wheels were subjected to rolling contact tests in the rail test rig, part of the wheel could likely have an increased tendency to reach rolling-contact fatigue failure prematurely due to high ratcheting rates. It is this was likely the case, then the data obtained would possess low accuracy when attempting to model and predict rail surface behaviour.

These observations provide motivation to improve rail material modelling by considering the variations that occur depending on the location from which the samples are taken, ultimately leading increased reliability of simulation and modelling results.

4. Conclusion

From the experiment analysis of the uniaxial stress controlled test and hardness test of the AS1085.1 rail steel, following conclusions:

1. Experiment approached is very useful for constitutive modelling of the cyclic hardening, softening and rail surface wear mechanism simulation.
2. Rectangular shape specimen provides more accurate data compared to cylindrical test coupons where material inhomogeneity existed.
3. This study shown that the rail disc obtained from the rail head for twin disc test rig, more prone to leave surface defects compared to rail surface.

However, this research has thrown up many questions in need of further investigation about how sampling has to be made and what rectification need to be made in the simulation process

Rectangular shaped specimens will able to make better justification on the rail surface material parameters with accurate test coupon design. The generalisability of these results is subject to certain limitations. For instance, these coupons couldn't be used to identify torsion parameters. The reasonable approach to tackle this issue on twin disc rail sample could be to forge them according to the standard specification and rail surface hardening condition.

5. Acknowledgements

This investigation has been performed within the Material laboratory in the Queensland University of Technology The Author would like to thank to Gregory Paterson and Sanjleena Singh for their assistance and guidance succeed this research.

6. References

1. J. Kirk, , "Fortescue opens the world's heaviest haul railway," Railway Gazette International., July 2008: p. 427.
2. C.L. Pun, and Q. Kan. "Ratchetting Behaviour of High Strength Rail Steel under Uniaxial and Biaxial Cyclic Loadings," in *ICF13*. 2013.
3. D.D. Hagarty, " A Short History of Railway Track in Australia - 1 New South Wales." Australian Railway Historical Society Bulletin, February 1999: p. 55–67.
4. A. Kapoor, J.H. Beynon, D.I. Fletcher, and M. Loo-Morrey. "Computer simulation of strain accumulation and hardening for pearlitic rail steel undergoing repeated contact," 2004. Professional Engineering Publishing Ltd.
5. A. Kapoor, D.I. Fletcher, F.J. Franklin, G. Vasic, and L. Smith. "Rail-wheel contact research at the University of Newcastle." in 11th International Conference on Fracture 2005, ICF11, March 20, 2005 - March 25, 2005. 2005. Turin, Italy: International Congress on Fracture.
6. J.W. Ringsberg," Life prediction of rolling contact fatigue crack initiation,"International Journal of Fatigue, 2001. 23(7): p. 575-586.
7. W. Tyfour, J. Beynon, and A. Kapoor," The steady state wear behaviour of pearlitic rail steel under dry rolling-sliding contact conditions,"Wear, 1995. 180(1): p. 79-89.
8. W. Tyfour, J. Beynon, and A. Kapoor," Deterioration of rolling contact fatigue life of pearlitic rail steel due to dry-wet rolling-sliding line contact,"Wear, 1996. 197(1): p. 255-265.
9. J. Seo, S. Kwon, H. Jun, and D. Lee. "Rolling contact fatigue of white etching layer on pearlite steel rail," 2010. Laubisrutistr.24, Stafa-Zuerich, CH-8712, Switzerland: Trans Tech Publications Ltd.

10. G.Z. Kang, , Q. Gao, X.J. Yang, and Y.F. Sun, "Strain cyclic characteristics and ratcheting of U71Mn rail steel under uniaxial loading," Acta Metallurgica Sinica (English Letters), 2000. 13(3): p. 893-900.
11. X. Yang, "Low cycle fatigue and cyclic stress ratcheting failure behavior of carbon steel 45 under uniaxial cyclic loading," International journal of fatigue, 2005. 27(9): p. 1124-1132.
12. A. Standard, "E466. Standard practice for conducting force controlled constant amplitude axial fatigue tests of metallic materials," West Conshohocken, PA: ASTM International, 2007.
13. H. Sunwoo, M. Fine, M. Meshii, and D. Stone, "Cyclic deformation of pearlitic eutectoid rail steel. Metallurgical Transactions,"A, 1982. 13(11): p. 2035-2047.